



Dehydrogenation process of AlH₃ observed by TEM



Yuki Nakagawa^{a,*}, Shigehito Isobe^{a,b}, Yongming Wang^a, Naoyuki Hashimoto^a, Somei Ohnuki^a, Liang Zeng^c, Shusheng Liu^c, Takayuki Ichikawa^c, Yoshitsugu Kojima^c

^a Graduate School of Engineering, Hokkaido University, N-13, W-8, Sapporo 060-8278, Japan

^b Creative Research Institution, Hokkaido University, N-21, W-10, Sapporo 001-0021, Japan

^c Institute for Advanced Materials Research, Hiroshima University, 1-3-1 Kagamiyama, Higashi-Hiroshima 739-8530, Japan

ARTICLE INFO

Article history:

Available online 27 February 2013

Keywords:

Hydrogen storage materials
AlH₃
TEM

ABSTRACT

Dehydrogenation processes of α - and γ -AlH₃ were investigated by *in situ* transmission electron microscopy observations. The relationship between Al₂O₃ thickness and dehydrogenation kinetics was also clarified. The initial shape of α -AlH₃ particle was cubic and that of γ -AlH₃ particle was rod-shaped. The process of γ -AlH₃ was quite similar with α -AlH₃. The precipitation and growth of Al was observed in both processes. The dehydrogenation kinetics did not depend on Al₂O₃ thickness. It was found that milling effect on the dehydrogenation kinetics was larger than doping effect. The dehydrogenation process was discussed in terms of both microscopic and kinetic studies.

© 2013 Elsevier B.V. All rights reserved.

1. Introduction

AlH₃ is a promising hydrogen storage material because of its high gravimetric and volumetric densities (10.1 mass% and 149 kg H₂/m³, respectively) [1]. It also desorbs hydrogen in a relatively low temperature range (100–200 °C) following the simple reaction (AlH₃ → Al + 3/2 H₂). α -AlH₃ is the most stable phase among the various crystalline structures of AlH₃ [2]. Baranowski et al. reported an estimated equilibrium H₂ pressure of 1 GPa at 25 °C according to the thermodynamic values taken from the report by Sinke et al. [3,4]. This value indicates that α -AlH₃ can spontaneously desorb hydrogen at room temperature. However, it has been suggested that the Al₂O₃ films on surface of AlH₃ particles inhibit the spontaneous dehydrogenation at room temperature [5]. Graetz et al. suggested that the enhanced stabilization of Dow's α -AlH₃ was primarily attributed to a thick surface oxide film [6]. They also stated its stabilization mechanism remains unknown. Kato et al. investigated the surface change of α -AlH₃ during the dehydrogenation by means of *in situ* X-ray photoelectron spectroscopy [7]. They proposed the dehydrogenation mechanism including the effect of Al₂O₃ film. They claimed that dehydrogenation only starts when the oxide film breaks up due to thermal expansion of the bulk AlH₃. In this way, Al₂O₃ film seems to play an important role in the kinetics. However, its exact role has not been clarified yet. Microscopic studies about the dehydrogenation

process of α -AlH₃ were performed by some groups. Ikeda et al. observed the precipitation and growth of Al particles inside the AlH₃ particles [8]. Muto et al. determined the surface films on AlH₃ particles as amorphous Al₂O₃ with a thickness of 3–5 nm by means of electron energy-loss spectroscopy [9]. However, the dehydrogenation process of γ -AlH₃ was not discussed in these microscopic studies. Dehydrogenation property of γ -AlH₃ was studied by some groups [10–12]. Graetz et al. reported the faster dehydrogenation kinetics of γ -AlH₃ than that of α -AlH₃ in the low temperature range (~100 °C) [11]. In this paper, our purpose is to investigate the dehydrogenation processes of α - and γ -AlH₃ in nanoscale by means of *in situ* transmission electron microscopy (TEM) observations. From the microscopic observations and kinetic studies, the relationship between Al₂O₃ thickness and dehydrogenation kinetics was also clarified.

2. Experimental procedures

AlH₃ was prepared by the chemical reaction between LiAlH₄ and AlCl₃ in ether solution [2]. Hand-milled sample was prepared by grinding AlH₃ for 5 min in an agate mortar under Ar atmosphere. Ball-milled and doped samples were prepared by ball-milling under 0.1 MPa Ar for 1 h. Ball-milling processes were performed by using a planetary ball-mill apparatus (Fritsch Pulverisette 7 at 200 rpm), with 18 stainless steel balls (7 mm in diameter) and 300 mg samples (ball:powder ratio = 64:1, by mass). Powder X-ray diffraction (XRD, Philips, X'Pert-Pro) was performed with Cu K α radiation. Thermogravimetry and differential thermal analysis (TG-DTA, Bruker, 2000SA) was performed with a heating rate of 2 °C/min under helium gas flow rate of 300 mL/min. Transmission electron microscopy (TEM, JEOL, JEM-2010) observations were carried out at 200 kV. The samples were dispersed on a molybdenum microgrid mesh for *in situ* TEM observations. A heating holder was required to heat samples in the TEM column.

* Corresponding author. Tel./fax: +81 11 706 6772.

E-mail address: y-nakagawa@eng.hokudai.ac.jp (Y. Nakagawa).

3. Results and discussion

3.1. Dehydrogenation process observed by TEM

The XRD profiles of AlH_3 before and after ball milling are shown in Fig. 1. We assigned the existence of $\alpha\text{-AlH}_3$ and small amount of $\gamma\text{-AlH}_3$ before and after ball milling. The temperature gradient in the reaction container during the sample synthesis would form the small amount of $\gamma\text{-AlH}_3$. It seemed that the profiles before and after ball milling almost did not change. Fig. 2 shows the dehydrogenation processes of $\alpha\text{-AlH}_3$ and $\gamma\text{-AlH}_3$ observed by TEM. $\alpha\text{-AlH}_3$ particles were found to have cubic morphology as shown in Fig. 2a. We observed Al_2O_3 films with a thickness of ~ 5 nm on surface of $\alpha\text{-AlH}_3$ particles. From the electron diffraction (ED) pattern,

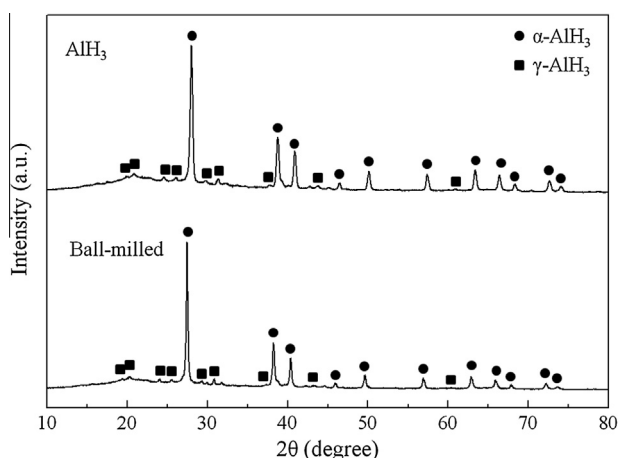


Fig. 1. Powder X-ray diffraction (XRD) profiles of AlH_3 particles.

the spots of $\alpha\text{-AlH}_3$ were assigned. As shown in Fig. 2b, both $\alpha\text{-AlH}_3$ and Al phases were assigned from the ED pattern, which was taken after 5 min. This suggests that the dehydrogenation partially occurs on surface of AlH_3 particles by electron beam exposure. From the bright field image, nanoscale (~ 1 nm) Al particles were observed inside single crystals of $\alpha\text{-AlH}_3$. Fig. 2c was taken after heating at 150°C for 30 min. From the ED pattern, only Al phase was assigned. Al particles grew to the large particles of size 50–100 nm by agglomeration. From these results, the precipitation and growth of Al particles were observed during the dehydrogenation process. The process of $\gamma\text{-AlH}_3$ was quite similar to that of $\alpha\text{-AlH}_3$. $\gamma\text{-AlH}_3$ formed aggregate of small rod-shaped particles as shown in Fig. 2d. $\gamma\text{-AlH}_3$ particles were also covered with thin Al_2O_3 films (~ 5 nm). During the dehydrogenation process, coexistence of $\gamma\text{-AlH}_3$ and Al phase was assigned as shown in the ED pattern of Fig. 2e. Finally, it decomposed into Al particles of size 10–100 nm as shown in Fig. 2f.

3.2. Al_2O_3 thickness and the dehydrogenation kinetics

In order to investigate the role of Al_2O_3 film on dehydrogenation kinetics, we changed Al_2O_3 thickness by exposing particles to air. The TEM images of Al_2O_3 films on AlH_3 particles are shown in Fig. 3. Fig. 4a shows the relationship between Al_2O_3 thickness and exposure time. Al_2O_3 thickness was increased with increasing the exposure time. It seemed that Al_2O_3 thickness was increased by diffusion-controlled growth as shown in Fig. 4a. Fig. 4b shows the relationship between the peak temperature of dehydrogenation and exposure time. The peak temperature remained almost constant after exposing to air. This result suggests that the dehydrogenation kinetics does not depend on Al_2O_3 thickness. In other words, it suggests that hydrogen diffusion through Al_2O_3 film is not the rate-limiting step. This result is in good agreement with the report by Kato et al. [7]. In addition, the peak temperature was

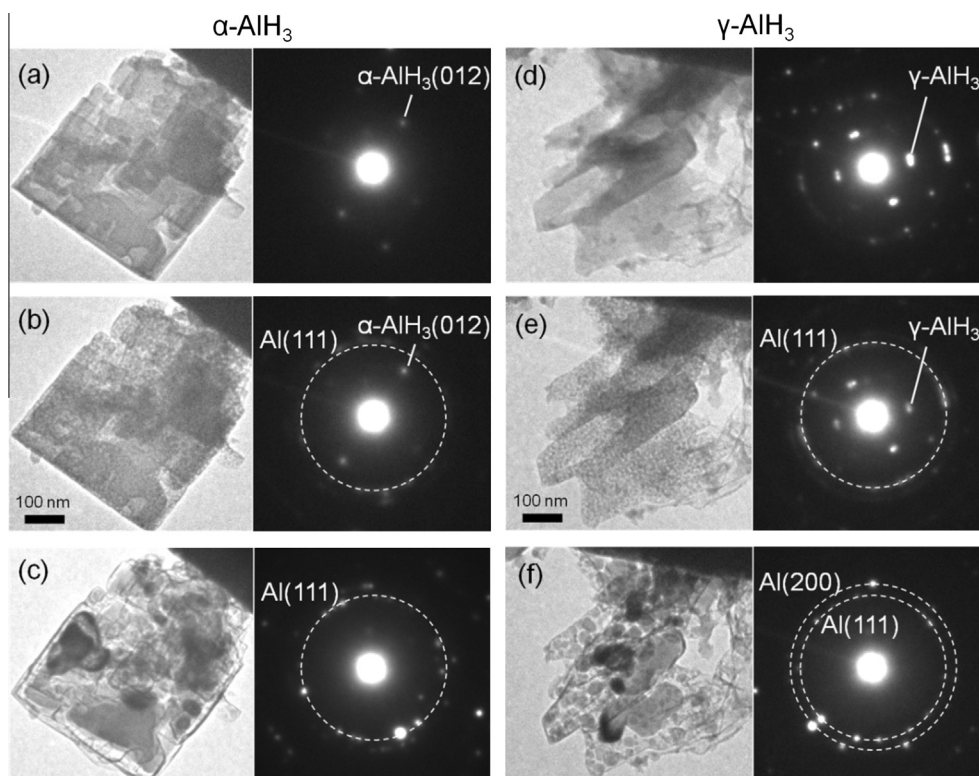


Fig. 2. TEM images and electron diffraction patterns of $\alpha\text{-AlH}_3$ (a–c) and $\gamma\text{-AlH}_3$ (d–f), which were taken (a and d) at the beginning of observation, (b and e) after 5 min, and (c and f) after heating (150°C , 30 min).

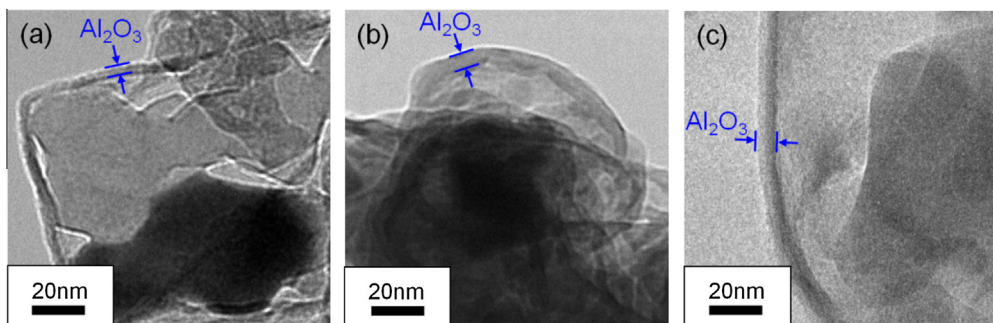


Fig. 3. The TEM images of Al_2O_3 films on AlH_3 particles; (a) without exposure to air, (b) 1 day exposure to air, and (c) 7 days exposure to air.

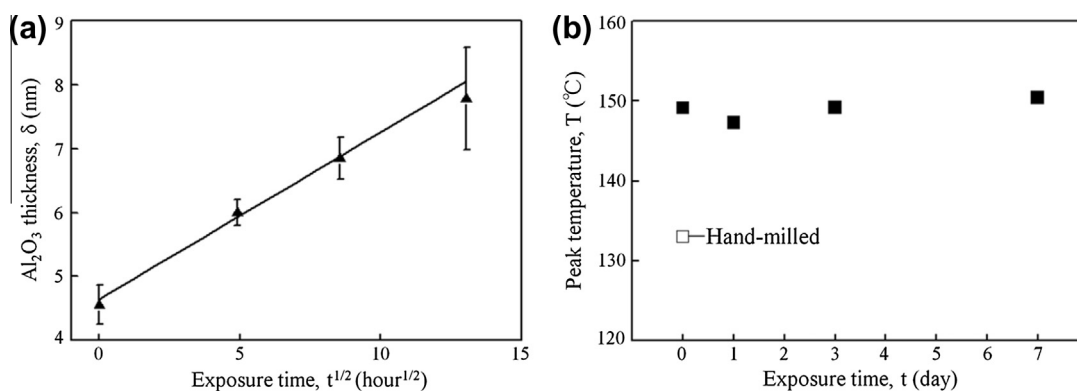


Fig. 4. The relationship between (a) Al_2O_3 thickness and exposure time and (b) peak temperature of dehydrogenation and exposure time. The peak temperature of dehydrogenation was derived by DTA profiles.

significantly decreased by hand milling under Ar atmosphere as shown in Fig. 4b. An increase of oxide free surfaces would enhance the dehydrogenation kinetics. From these results, it is suggested that the existence of Al_2O_3 film delays the dehydrogenation kinetics.

3.3. The effect of milling and doping on dehydrogenation kinetics

The dehydrogenation kinetics of AlH_3 was investigated in detail by the derivatives of TG curves. Fig. 5a shows the derivatives of TG curves of pure AlH_3 and ball-milled one. Two peaks were found in the profile of pure AlH_3 . The first peak at 128 °C would be ascribed to the dehydrogenation from γ - AlH_3 . The second peak at 145 °C would correspond to the dehydrogenation from α - AlH_3 .

This result is in good agreement with the report by Maehlen et al. [12]. Ball milling resulted in the decrease of dehydrogenation temperature by 10–20 °C. In addition, we investigated the doping effect with AlH_3 on its dehydrogenation kinetics. The results are shown in Fig. 5b. Al was doped as a metal catalyst on surface recombination of hydrogen. LiAlH_4 or LiBH_4 was doped as a reductant of Al_2O_3 film. Ni was doped as a reference. As shown in Fig. 5b, no dopant was effective to the dehydrogenation kinetics of AlH_3 . The result of LiAlH_4 doping was different with the report by Sandrock et al. [5], which mentioned that LiAlH_4 acted to enhance the kinetics. The different synthesis of AlH_3 may result in the different results. As a result, it was suggested that milling effect was significantly larger than doping effect on dehydrogenation kinetics of AlH_3 .

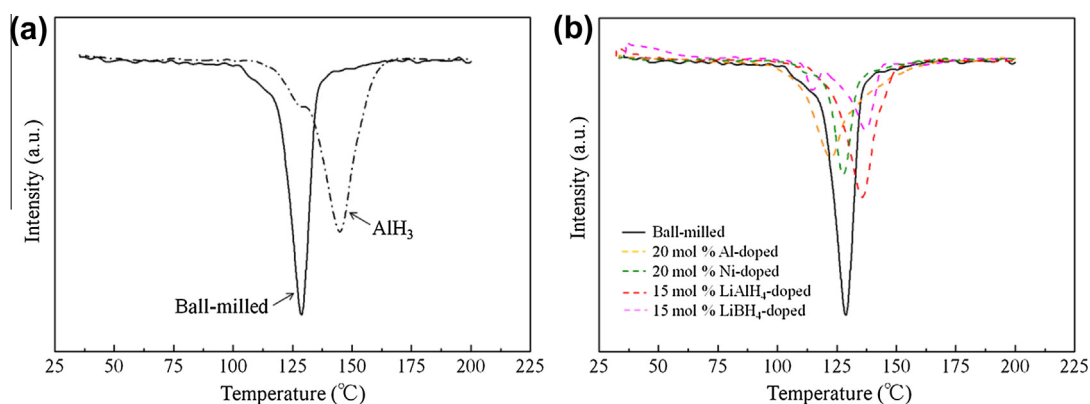


Fig. 5. The derivatives of TG curves of AlH_3 samples. (a) shows ball milling effect and (b) shows doping effect. Milled and doped samples were ball-milled at 200 rpm for 1 h.

4. Conclusion

In this work, we investigated the dehydrogenation processes of α - and γ -AlH₃. The initial shape of α -AlH₃ particle was cubic and that of γ -AlH₃ particle was rod-shaped. The precipitation and growth of Al was observed in both processes. The dehydrogenation kinetics did not depend on Al₂O₃ thickness in the 4.6–7.8 nm range. The existence of Al₂O₃ film would delay the kinetics. Milling effect on dehydrogenation kinetics was found to be significantly larger than doping effect. An increase of oxide free surfaces by milling would enhance the kinetics.

Acknowledgement

This work has been partially supported by HYDRO STAR (NEDO) and L-station (Hokkaido University).

References

- [1] G. Sandrock, J. Reilly, J. Graetz, W.M. Zhou, J. Johnson, J. Wegrzyn, Appl. Phys. A 80 (2005) 687–690.
- [2] F.M. Brower, N.E. Matzek, P.F. Reigler, H.W. Rinn, C.B. Roberts, D.L. Schmidt, J.A. Snover, K. Terada, J. Am. Chem. Soc. 98 (1976) 2450–2453.
- [3] B. Baranowski, M. Tkacz, Z. Phys. Chem. 135 (1983) 27–38.
- [4] G.C. Sinke, L.C. Walker, F.L. Oetting, D.R. Stull, J. Chem. Phys. 47 (1967) 2759–2761.
- [5] G. Sandrock, J. Reilly, J. Graetz, W.M. Zhou, J. Johnson, J. Wegrzyn, J. Phys. Chem. 421 (2006) 185–189.
- [6] J. Graetz, J.J. Reilly, V.A. Yartys, J.P. Maehlen, B.M. Bulychev, V.E. Antonov, B.P. Tarasov, I.E. Gabis, J. Alloys Comp. 509S (2011) S517–S528.
- [7] S. Kato, M. Biemann, K. Ikeda, S. Orimo, A. Borgschulte, A. Züttel, Appl. Phys. Lett. 96 (2010) 051912.
- [8] K. Ikeda, S. Muto, K. Tatsumi, M. Menjo, S. Kato, M. Biemann, A. Züttel, C.M. Jensen, S. Orimo, Nanotechnology 20 (2009) 204004.
- [9] S. Muto, K. Tatsumi, K. Ikeda, S. Orimo, J. Appl. Phys. 105 (2009) 123514.
- [10] S. Orimo, Y. Nakamori, T. Kato, C. Brown, C.M. Jensen, Appl. Phys. A 83 (2006) 5–8.
- [11] J. Graetz, J. Reilly, J.G. Kulleck, R.C. Bowman, J. Alloys Comp. 446–447 (2007) 271–275.
- [12] J.P. Maehlen, V.A. Yartys, R.V. Denys, M. Fichtner, C. Frommen, B.M. Bulychev, P. Pattison, H. Emerich, Y.E. Filinchuk, D. Chernyshov, J. Alloys. Comp. 446–447 (2007) 280–289.